



Sugarcane trash-derived nanocrystalline cellulose: a sustainable approach with mild chemical pretreatment and comprehensive characterisation

Milind Joshi · Sampatrao Manjare

Received: 17 September 2023 / Accepted: 9 April 2024 / Published online: 19 April 2024
© The Author(s), under exclusive licence to Springer Nature B.V. 2024

Abstract Cellulose-rich sugarcane trash (SCT) biomass, an important agricultural residue generated in large quantities every year, was used as a potential feedstock for cellulose extraction in micro and nano form. Initially, the cellulose microfibrils were isolated from the SCT by a two-step chemical treatment process (alkali pretreatment with sodium hydroxide followed by hydrogen peroxide bleaching) at different operating parameters. The microfibrils were then converted into the nanoscale by acid hydrolysis. The quantification of the raw and chemically treated SCT was carried out by the Van Soest method to learn their chemical composition. Different characterisation techniques such as Fourier Transform Infrared spectroscopy (FTIR), Thermogravimetric Analysis (TGA), X-Ray Diffraction (XRD), Field Emission-Scanning Electron Microscopy (FE-SEM), and Transmission Electron Microscopy (TEM) were used for the analysis of surface functional groups, thermal stability, crystallinity index, surface morphology, and the internal structure of the raw as well as chemically treated SCT biomass respectively. The quantification results show the optimum process conditions for the alkali pretreatment as 5% (w/v) alkali (NaOH) concentration, 60 °C, and 12 h process time and for

bleaching as 20% H₂O₂ concentration, 80 °C, and 8 h process time. This produces material having 86.15% cellulose content. This indicates the effective removal of hemicellulose and lignin. For the acid hydrolysis reaction for converting cellulose microfibrils into nanocrystalline cellulose, the concentration of H₂SO₄ required was 40 wt.%, which is comparatively lower than that reported in the literature (~65 wt.%). The characterisation results highlight the progressive enrichment in the cellulosic groups, thermal stability, and crystallinity of the material with respect to the processing stages. There was a progressive enhancement in the crystallinity index of the sample observed with respect to the chemical treatment, with a maximum of up to 84.83% for the hydrolysed material. The XRD and TEM analysis confirms the presence of nanocrystalline cellulose (NCC) in the final hydrolysed sample.

Keywords Sugarcane trash · Renewable · Cellulose · Alkali pretreatment · Bleaching · Hydrolysis

Introduction

In the current scenario, the non-renewable and fossil-based sources alone fulfill almost all the raw materials and energy requirements for the process industries. As the demand and thus production of essential daily commodities increase with the growing population, the

M. Joshi · S. Manjare (✉)
Materials and Environmental Research Lab, Department of Chemical Engineering, BITS Pilani, K. K. Birla Goa Campus, Zuarinagar, Goa, India
e-mail: manjare@goa.bits-pilani.ac.in

utilisation of fossil-based sources also rises simultaneously. Due to the limited availability and rapid depletion rate, the excessive dependence on non-renewable fossil-based sources cannot be sustained in the long run. Furthermore, its use has a negative impact on the environment, resulting in air pollution, high greenhouse gas emissions in the atmosphere, global warming, and drastic climate changes (Ballesteros et al. 2006; Haghghi Mood et al. 2013; Baruah et al. 2018).

The application of renewable or bio-based sources to a great extent for material and energy needs is a feasible and optimistic solution to this problem. The implementation of lignocellulosic biomass (LCB) as a sustainable feedstock, which is the world's most abundant, highly renewable natural resource available, can reduce the dependence on non-renewable petroleum-based sources for the production of chemicals, energy, and materials to some extent (Hussain et al. 2017; Ning et al. 2021). The utilisation of LCB, which has significant potential as a sustainable feedstock for manufacturing biomaterials, biochemical, and biofuels for energy without compromising global food security, is one promising strategy in this area (Zoghliami and Paës 2019). It also becomes the most cost-effective because it is extensively available at a cheap rate. The key ingredients present in LCB are cellulose, hemicellulose, and lignin, along with a minimal quantity of extractives hydrocarbon (such as starch, water, lipids, essential oils, resins, proteins, and simple sugars) and inorganic ash (mainly comprising silica), which are scattered along the cell walls of biomass (Yu et al. 2021; Yogalakshmi et al. 2022). LCB includes crops and residues, forest products such as hardwood and softwood, algae, grass, and other organic elements.

Crop residues, such as rice straw, rice husks, wheat straw, corncobs, sugarcane bagasse, mustard plant waste, sugarcane trash, and so on, are significant sources of waste biomass in the agricultural sector. The type of source primarily determines the chemical composition of LCB. The generation of residual biomass in agriculture-dominated economies like India is a major source of concern due to the challenge of disposal. The typical way to dispose of the leftovers is to burn them in an open field, which decreases the massive amounts of residue. However, burning the waste produces a significant amount of air pollution. This pollutant can potentially harm the respiratory systems of people in the area. As a result, it is critical to make use of valuable components like cellulose,

which can be found in significant quantities in so-called agricultural waste.

The isolation of cellulose, hemicellulose and lignin from the complicated hierarchical structure of LCB is required for its valorisation for various applications. The cellulose, with a crystalline nature, which is embedded in a matrix of polymers such as lignin and hemicellulose, causes the recalcitrant behaviour of LCB. This recalcitrance of LCB leads to the major obstacle in the isolation of its valuable components. Pretreatment of biomass is regarded as an important step in overcoming this barrier since it allows the separation of cellulose by solubilising non-cellulosic components (Lee et al. 2014). The various chemical pretreatment methods that separate cellulose and hemicellulose from other non-cellulosic components, like lignin, are reported in the literature. Some of them are acid pretreatment, alkali pretreatment, wet oxidation, organosolv process, ionic liquid pretreatment, and deep eutectic solvents (Maryana et al. 2014; Kumari and Singh 2018; Baruah et al. 2018; Owonubi et al. 2021).

The cellulose thus extracted from different LCB sources and its transformation into the nanocellulose (nanofibrillated cellulose (NFC), nanocrystalline cellulose (NCC), and bacterial nanocellulose (BNC)) has a broad spectrum of applications due to its properties like biodegradability, good thermal stability, biocompatibility, and high reinforcing ability (Mishra et al. 2019; Khan et al. 2021). Nanocelluloses can be used for applications as reinforcing filler for polymeric and elastomeric composites, in packaging applications for preparing biodegradable composites, in pharmaceutical industries for wound healing and controlled drug release, as an adsorbent for removal of microplastics from wastewater streams, in food industry as a food additive, emulsifier, stabilizer, thickener, and anti-caking agents; in cosmetic industry as excipient, binder, and adsorbent; and so on (Seddiqi et al. 2021; Basta and Lotfy 2023a, b).

The sugarcane trash (SCT) is a cellulose-rich (40–45% cellulose content) agriculture residue left in the field after harvesting and can be used as a potential biomass for the extraction and enrichment of cellulose (Powar et al. 2022). As per UN data, sugarcane (*Saccharum officinarum*) is an important cash crop cultivated worldwide that holds a substantial stake in that country's economy, accounting for almost 20% (1.9 billion tonnes) of the global production of primary crops. According to the Press Information

Bureau, Government of India, in the sugar season 2021–22, India becomes the World's largest producer, consumer, and second largest exporter of sugar. In 2021–22, sugarcane production in India was more than 5000 lakh metric tonnes (LMT) over almost 5.15 million hectares. The increase in sugarcane production also generates a huge amount of waste residues from its harvesting to final processing in the sugar mill in the form of dry leaves and tops (trash), bagasse, press mud, and molasses (Singh et al. 2021). Sugarcane bagasse is currently used as a fuel for boilers due to its high energy content (calorific value), but sugarcane trash is not popular as a boiler fuel despite having comparable energy content to that of bagasse because of its high mineral contents, and thus generally burned in the open field by the farmers which causes severe air pollution in the surrounding area (Chotirotasukon et al. 2019).

The research so far has been focusing mainly on the utilization of sugarcane bagasse for the isolation of cellulose for producing biofuels through enzymatic saccharification. Various pretreatment methods that have been employed are extrusion (Moro et al. 2017), microwave-based (Intanakul et al. 2003), ultrasound (Sun et al. 2004; Velmurugan and Muthukumar 2011), supercritical CO₂ (Benazzi et al. 2013), liquid hot water (Hongdan et al. 2013), alkali (Talha et al. 2016; Nosratpour et al. 2018), Organosolv (Zhang et al. 2018), and deep eutectic solvent (Kumar et al. 2021).

On the other hand, very limited studies are available on sugarcane trash as the feedstock material to produce bioenergy, biochemical, and biomaterials. (Sindhu et al. 2014), performed an alkali pretreatment on sugarcane tops with 3% NaOH concentration at 121 °C for 1 h in an autoclave. The response surface method was used based on Box- Behnken design for the optimization of the enzymatic saccharification. The physico-chemical characterisation of raw and pre-treated sugarcane tops was carried out using XRD, FTIR, and SEM. The results reveal that, due to alkali pretreatment, 77.5% sugar recovery was achieved with almost 90% lignin removal. In another study reported by (Chotirotasukon et al. 2019), sugarcane trash fractionation was carried out by the organosolv method with aqueous glycerol catalysed by oxalic acid followed by acetone treatment for mild delignification. The different reaction parameters were varied, such as temperature (150–170 °C), the concentration of glycerol (20– 80% v/v),

and catalyst (oxalic acid) concentration (75– 300 mM) to see the effect on efficiency and selectivity of the reaction. The result shows 71.7% cellulose was recovered with the removal of 96.8% hemicellulose and 83.9% lignin at the optimal reaction conditions of 80% v/v glycerol concentration at 170 °C and oxalic acid concentration of 300 mM. In addition, the recovered lignin shows a 73.7% yield with 94.6% purity.

Similar studies were reported on the pretreatment of sugarcane trash (dry leaves or tops/ straws) to improve glucose recovery after enzymatic hydrolysis in bioethanol production by using different methods such as waste glycerol-assisted transition metal and alkali pretreatment (Raghavi et al. 2016), steam explosion pretreatment (Oliveira et al. 2013), dilute acid and alkali pretreatment (Jutakanoke et al. 2012), and biological pretreatment (Singh et al. 2008).

The literature survey revealed that the information on cellulose extraction from SCT is very scanty and needs more investigation to optimize the extraction process conditions. Similarly, among the pretreatment methods mentioned above, the chemical pretreatment method has its distinct advantages like selectivity in removing hemicellulose and lignin without degrading the cellulose structure, low thermal and mechanical energy consumption, use of mild, non-corrosive, and non-hazardous chemicals, and environmental friendliness.

In view of the above, the present research work was undertaken to isolate the cellulose from the sugarcane trash (SCT) biomass by using a chemical pretreatment method. This chemical pretreatment was divided into two steps, alkali treatment with sodium hydroxide (NaOH) followed by bleaching with hydrogen peroxide due to its chlorine-free nature, strong oxidising ability, and environmental friendliness (Mussatto et al. 2008). This pretreatment was carried out by varying process conditions such as concentrations of alkali (NaOH) and bleaching agent (H₂O₂), temperature, and process time. The use of these chemicals in the pretreatment process will not generate any harmful waste. Acid hydrolysis was performed on the extracted cellulose microfibrils using sulphuric acid to convert them into nanocrystalline cellulose (NCC) by removing its amorphous portion.

Materials and methods

Materials

The sugarcane trash biomass was obtained from the local farm of the Sangli district of Maharashtra state in India. The chemicals required for the pretreatment of biomass and for the quantification of material at different treatment stages, such as sodium hydroxide (NaOH, 98% purity), hydrogen peroxide (H₂O₂, 30% solution), sodium lauryl sulphate, di-sodium tetraborate (Borax), ethylenediamine tetra acetic acid (EDTA), disodium hydrogen o-phosphate, cetyltrimethylammonium bromide (CTAB), sulphuric acid (H₂SO₄, 98%), and acetone were purchased from Optech Enterprises, Goa (India).

Experimentation

Biomass preparation

Initially, the sugarcane trash biomass was washed with plenty of water to remove dirt particles on the surface and then dried in sunlight for 24 h, followed by hot air oven drying at 60 °C until moisture content in the biomass becomes constant. Then, the long trash particles were cut to a smaller size, followed by grinding to a fine powder using the conventional grinder and sieved using a 600- μ m mesh screen. This powder was stored in a sealed container at room temperature until its use for characterization and pretreatment.

Alkaline pretreatment

The alkaline pretreatment was carried out at various concentrations of sodium hydroxide (NaOH) solution as 1%, 3%, 5%, 7% and 9% (w/v); for different temperatures as ambient temperature (\approx 27 °C), 40 °C, 60 °C, and 80 °C; and for processing time as 4, 8, 12, 16, 20, and 24 h. The solid-to-liquid ratio used was 1:25.

The operating parameters were selected based on the fact that, at low alkali concentrations (<10%) and low temperature (<100 °C), the β (1,4) glycosidic bonds within the cellulose structure remain alkali-stable, and thus the changes in cellulose structure become negligible (Knill and Kennedy 2003; Modenbach and Nokes 2014).

After completion of the pretreatment cycle at the given conditions, the solid residue was recovered through vacuum filtration under the continuous water wash to neutralize the p^H of the sample and until the colourless filtrate was produced. After the filtration step, the solid residue was kept in a hot air oven for drying at 60 °C until the constant weight of the solid was obtained. A part of this solid residue was used for the compositional analysis, and the remaining part was further treated with hydrogen peroxide.

Bleaching with hydrogen peroxide

The dried solid residue obtained after the alkali pretreatment at the optimum process conditions undergoes a bleaching process using hydrogen peroxide (H₂O₂) at three different concentrations: 10%, 20%, and 30% (w/v). The temperature varies from ambient temperature (\approx 27 °C) to 80 °C, whereas processing time was set up to 24 h with intervals of 4 h, similar to that of alkaline pretreatment. The solid-to-liquid (S: L) ratio selected here was 1:20.

After this bleaching step, the slurry was washed with distilled water, vacuum filtered, and dried in a hot air oven at 60 °C until constant weight was achieved. The cellulose-rich dry solid (cellulose microfibrils) was stored in a sealed container before further analysis.

Nanocrystalline cellulose preparation by acid hydrolysis

The nanocrystalline cellulose (NCC) was obtained by the acid hydrolysis of the cellulose microfibrils. At the higher concentration of H₂SO₄ solution (50 or 65 wt.%), the bleached SCT fibers (cellulose microfibrils) get decomposed and resulted in a black slurry. Thus the cellulose microfibrils were reacted with 40 wt.% concentrated sulphuric acid (H₂SO₄) solution with S: L = 1:20 at 45 °C for 90 min. Then, the known quantity of chilled distilled water was quickly poured into the reaction mixture to stop the reaction. The entire slurry was washed frequently (4 to 5 times) with distilled water to remove the traces of H₂SO₄ with simultaneous centrifugation at 5000 rpm, for 15 min, and at 10 °C. After the final water wash, the slurry was centrifuged, and the white solid cake obtained was dried in the hot air oven at 60 °C until constant weight was obtained.

The NCC powder thus produced (hydrolysed sample) was stored in an air-tight container and analysed with different characterisation techniques.

Characterisation

Determination of chemical composition

The chemical composition of raw sugarcane trash, alkali treated, and bleached fibers of sugarcane trash was determined using the Van- Soest method (Van Soest et al. 1991) to study the effect of different process parameters such as concentrations of alkali and bleaching agents, temperature, and time on cellulose enrichment. This method consists of three steps: (i) determination of Neutral Detergent Fiber (NDF), (ii) determination of Acid Detergent Fiber (ADF), and (iii) determination of Acid Detergent Lignin (ADL). With this method, it is possible to calculate the amount of major components present in the given biomass sample such as cellulose, hemicellulose, lignin, extractives, and inorganic matter.

NDF and ADF can be determined by treating the given biomass sample sequentially with a neutral detergent solution (distilled water, sodium lauryl sulphate, Borax, EDTA, and disodium hydrogen o-phosphate) and acid detergent solution (distilled water, CTAB, and 96% H₂SO₄) for 1 h at boiling temperature followed by washing (with hot water and acetone), filtration and drying till constant weight. Then, the sample was treated with 72% H₂SO₄ for 3 h, followed by filtration and drying. The dried sample was heated in a muffle furnace at 550 °C for 2 h, which gives the ADL value.

The following equations (Eqs. 1, 2 and 3) were used for the calculation of the lignocellulosic content of the given biomass sample:

$$\% \text{ Hemicellulose} = (\text{NDF} - \text{ADF}) \times 100 \quad (1)$$

$$\% \text{ Cellulose} = (\text{ADF} - \text{ADL}) \times 100 \quad (2)$$

$$\% \text{ Lignin} = \text{ADL} \times 100 \quad (3)$$

Fourier Transform Infrared (FTIR-ATR) analysis

Perkin Elmer spectrometer fitted with diamond crystals was used to record the Attenuated Total Reflection Fourier Transform Infrared (FTIR-ATR) spectra

of raw and treated (alkali-treated and bleached) biomass samples in the range of 4000–400 cm⁻¹ with 48 scans and at a resolution of 16 cm⁻¹.

Morphological analysis using FE-SEM

The morphological analysis of raw and treated SCT samples was done using Quanta FEG 250 Field Emission-Scanning Electron Microscopy (FE-SEM). Before analysis, all the samples were prepared with gold coating by using LEICA EM ACE 200 sputter coater. The effect of chemical treatment on the surface morphology of biomass samples was investigated by recording FE-SEM images at different magnifications.

Thermogravimetric analysis (TGA)

The thermal stability of the raw and treated sugarcane trash sample was analysed using TA Instruments Trios V5.2.2.47561 thermogravimetric analyser. During analysis, a heating rate of 20 °C/minute under a nitrogen atmosphere was maintained while heating the samples from 25 °C to 600 °C.

X-ray diffraction (XRD) analysis

The XRD analysis of sugarcane trash at different treatment stages was carried out using a Bruker D8 Advance X-Ray diffractometer at 40 kV, 40 mA with Cu- K α radiation ($\lambda = 1.5418 \text{ \AA}$). The data was gathered for the 2θ values between 5° and 50° at the scanning rate of 2°/minute. The crystallinity index (CrI) of the given sample was calculated as per the following Eq. 4 (Segal et al. 1959),

$$\text{Crystallinity index, CrI (\%)} = \frac{(I_{200} - I_{am})}{(I_{200})} \times 100 \quad (4)$$

where I_{200} is the maximum intensity of the lattice diffraction peak of crystalline material measured for 2θ angle between 22° to 23° (200 peak), and I_{am} is the minimum intensity of diffraction for amorphous material measured for 2θ between 18° to 19° (between the (1 $\bar{1}$ 0/110) peak and the (200) peak) in counts. Initially, a blank run was conducted at similar conditions as the biomass samples and the data thus obtained was subtracted from the diffractogram data and used in the calculation of CrI values.

Transmission electron microscopy (TEM)

TEM analysis of the hydrolysed sample was carried out by using 80 kV aberration-corrected Themis TEM in STEM-HAADF mode with a LaB6 electron source and super twin objective lens system in order to determine the dimensions of the particles present in the sample. The sample preparation was carried out before imaging by using a drop cast method, where a small drop of diluted solution of hydrolysed material was placed on a carbon-coated copper grid and allowed to dry at ambient temperature.

Results and discussion

Compositional analysis

The cellulose microfibers were extracted from SCT biomass by a two-step process of alkali pretreatment followed by peroxide bleaching by changing the different process variables, such as concentration of the reagent used (NaOH and H₂O₂), temperature, and

processing time. The effect of these variables on the extraction and enrichment of cellulose is summarised graphically in Figs. 1 and 2.

From Fig. 1, it is clear that the percentage of cellulose content of the given biomass increases with the concentration of NaOH from 1 to 5%, but beyond that, it remains almost constant. A similar trend is observed for the change in temperature from room temperature to 60 °C and for the change in processing time up to 12 h, that the cellulose enrichment is progressive, and then it becomes insignificant with further change in time and temperature.

The microfibers thus extracted from the raw SCT biomass by alkali pretreatment at the optimum conditions of 5% NaOH (w/v), 12 h, and 60 °C were further subjected to bleaching treatment with hydrogen peroxide (H₂O₂).

In the case of a bleaching operation, as shown in Fig. 2, the delignification and, hence, the cellulose enrichment increased with the concentration of H₂O₂ from 10 to 20%, temperature from room temperature to 80 °C, and time from 0 to 8 h, and further change in cellulose content with process parameters was negligible.

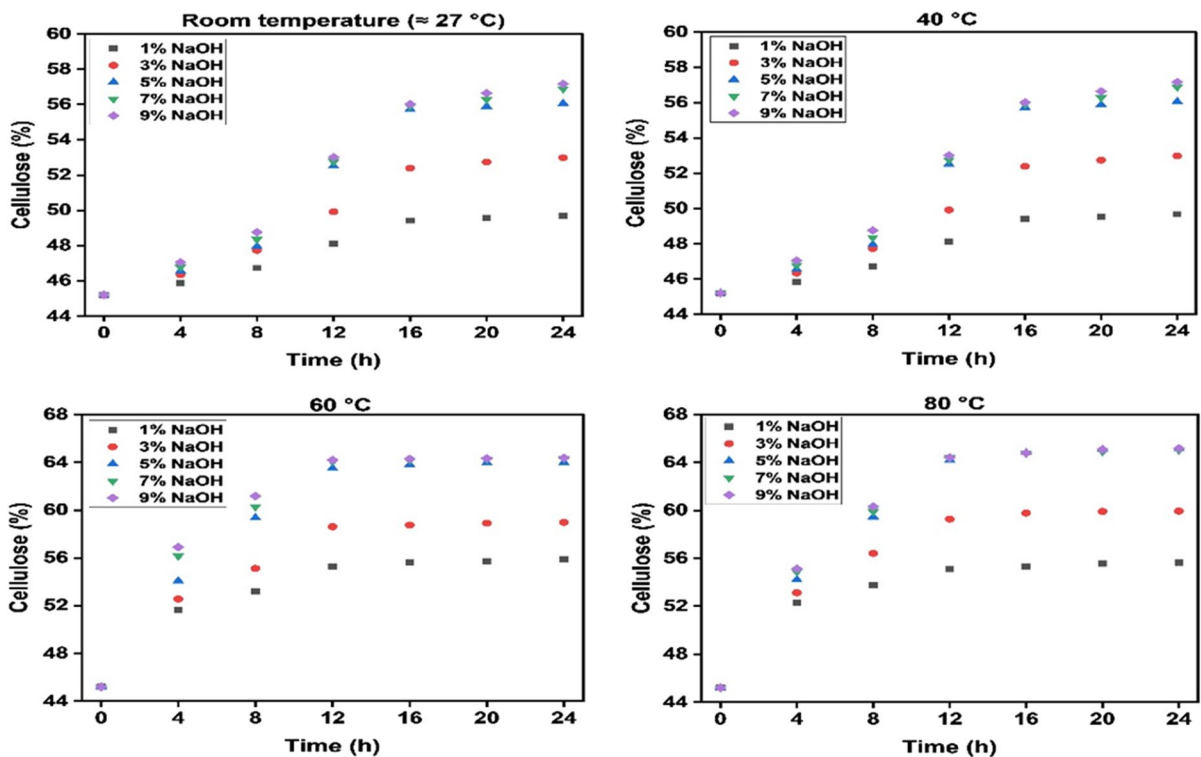


Fig. 1 Effect of NaOH concentration, process temperature, and time on the extraction of cellulose from raw SCT

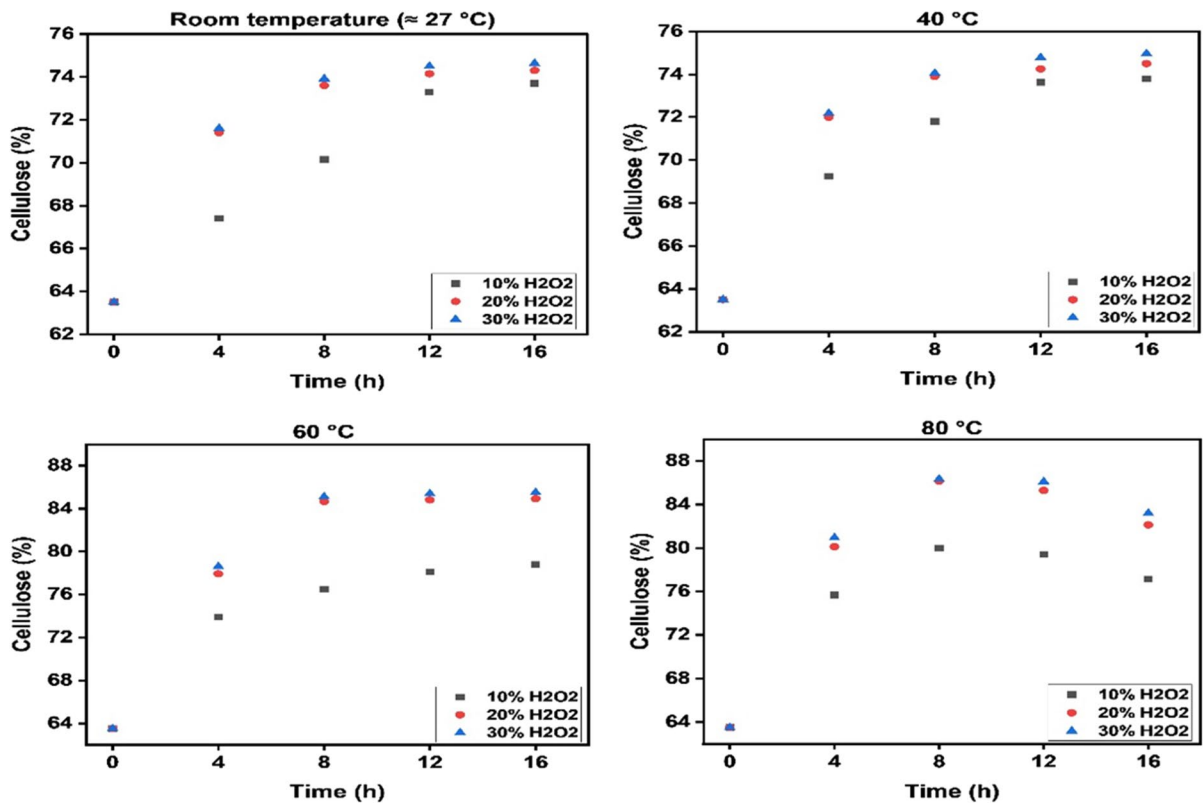


Fig. 2 Effect of H₂O₂ concentration, process temperature, and time on the enrichment of cellulose microfibers extracted from raw SCT biomass by alkali pretreatment at 5% NaOH (w/v), 12 h, and 60 °C

During the alkali pretreatment, NaOH primarily targets and ruptures the ester bond that exists between the lignin and hemicellulose, thereby isolating and solubilizing these components. The lignin fraction may get partially solubilised with the degradation of hemicellulose structure to a greater extent (Modenbach and Nokes 2014). The removal rate of hemicellulose and lignin increases with NaOH concentration and temperature initially and then becomes steady. This is why, beyond 5% NaOH concentration and 60 °C, the cellulose extraction and removal of hemicellulose and lignin becomes almost stable.

The bleaching process primarily targets the lignin content of the biomass through oxidation. The chromophores present in the lignin are responsible for the dark brown colour of any given biomass. Hydrogen peroxide reacts with these chromophores and converts them into benzoquinone derivatives through

an irreversible reaction. Thus, due to the bleaching with H₂O₂, a brown-coloured biomass material changes into colourless compounds (Li et al. 2015).

From Figs. 1 and 2, the optimum process conditions for alkali pretreatment were 5% NaOH concentration, 60 °C, and 12 h of processing, and for bleaching, it was 20% H₂O₂, 80 °C, and 8 h of processing produces the solids with 63.5% and 86.15% cellulose composition respectively. The detailed composition of the SCT samples at these optimum conditions with the standard deviation is represented in Table 1 below.

Further characterisation was conducted for the samples, which were alkali pretreated and bleached only at these optimum process conditions. At the same time, the acid hydrolysis of the bleached sample was carried out as per the conditions mentioned in the literature, such as 40 wt.% H₂SO₄ concentration, 45 °C, and 90 min of reaction time.

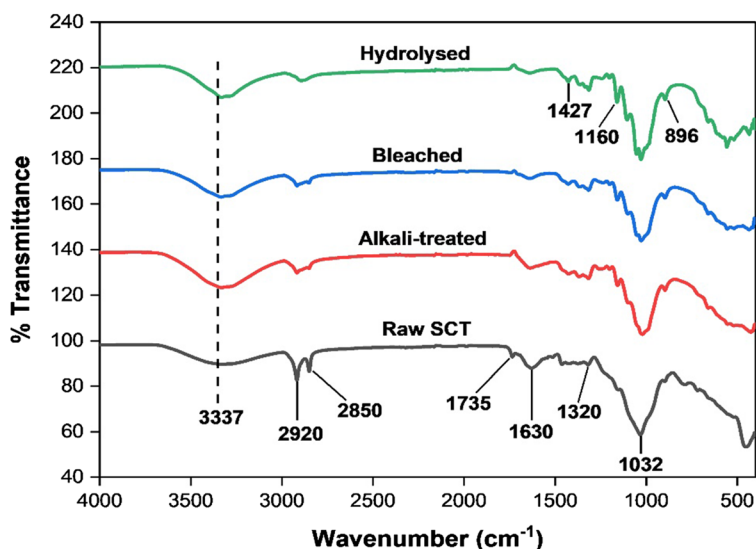
Table 1 Chemical composition of raw and treated SCT biomass at optimum process conditions

Treatment stage	Composition (%)				
	Cellulose	Hemicellulose	Lignin	Extractives	Inorganic matter
Raw	45.2 ± 0.09	23.81 ± 0.85	15.99 ± 0.1	12.15 ± 0.25	2.85 ± 0.05
Alkali treated	63.5 ± 0.15	9.85 ± 0.8	12.95 ± 0.08	11.13 ± 0.15	2.57 ± 0.02
Bleached	86.15 ± 0.25	5.2 ± 0.25	5.18 ± 0.05	1.18 ± 0.05	2.29 ± 0.02

Functional group analysis

The analysis of surface functional groups of raw and chemically treated SCT at different stages (raw, alkali treated, bleached, and hydrolysed SCT sample) through FTIR is presented in Fig. 3. The change in the functional groups, i.e., the composition of the material due to the chemical treatment, was identified by the change in infrared absorption. As seen in Fig. 3, for all the samples, the FTIR peak at 3337 cm^{-1} suggests the presence of cellulose as there is a stretching vibration of O–H bonds present in the OH group. The increase in the intensity of this peak indicates the enrichment of this cellulosic group concerning the chemical treatment. The peak observed at 2920 cm^{-1} represents the stretching vibrations of the C–H group present in the hemicellulose molecule (Enriquez et al. 2016). The intensity of this peak reduced gradually as there was a degradation of hemicellulose due to the pretreatment of SCT biomass. The FTIR peak at 1735 cm^{-1} indicates the C=O stretching vibrations of acetyl and uronic ester groups from hemicellulose and lignin (Sain and Panthapalakal 2006).

Similarly, the presence of ester bond linkages between lignin and hemicellulose is observed from the peak at 1630 cm^{-1} (Coelho de Carvalho Benini et al. 2017) for raw SCT, which becomes weaker as the treatment progresses. The bending vibration of C–O and C–H groups present in the aromatic rings of the polysaccharide can be observed through the vibration peaks at 1320 to 1375 cm^{-1} (NACOS et al. 2006). For all the sample stages, the major peak at 1032 cm^{-1} corresponds to the C–O–C pyranose ring skeletal vibration of cellulose (Ditzel et al. 2017; Oliveira et al. 2017). The increase in the intensity of this peak with the chemical treatment confirms the increase in the composition and crystallinity of the cellulose in the given sample (Elanthikkal et al. 2010; Wahib et al. 2022). In addition to this, another peak observed at 1160 cm^{-1} refers to the stretching vibration of the C–C ring present in the cellulose (Ditzel et al. 2017; Oliveira et al. 2017). The stretching of this peak is observed from the spectra of alkali pretreatment that further enhances in the bleached and hydrolysed sample, indicating the enrichment of

Fig. 3 FTIR spectra of raw and chemically treated SCT at different treatment stages

cellulosic groups in the treated sample compared to that of raw SCT.

For the spectra of hydrolysed sample, the peaks at 1427, 1032, and 896 cm^{-1} are typically related to CH_2 bending, C-O stretching, and C-H bending, respectively, which primarily represent the cellulose absorption peaks. A peak represents the typical cellulose structure at 896 cm^{-1} due to the β -glycosidic linkages of the glucose ring of the cellulose chain (Lamaming et al. 2015; Chieng et al. 2017).

In addition to this, the stretching vibration of the OH group is observed by a broad spectrum centered around 3337 cm^{-1} for the raw SCT sample. For alkali-treated and bleached SCT samples, the spectra show a redshift of OH bands to a lower frequency; however, the highest shifting is observed for the acid-hydrolysed sample, which signifies the removal of an amorphous section of the given sample (Basta and Lotfy 2023b).

Therefore, this FTIR analysis confirms that the chemical pretreatment was effective enough to progressively remove the non-cellulosic components as well as the amorphous region from the raw SCT sample, thereby enriching it with cellulosic groups.

Morphological analysis

The morphological analysis of raw and chemically treated SCT samples was conducted using the FE-SEM technique at the same magnification level. The images thus obtained are summarised in Fig. 4-A. These images clearly indicate the change in morphology of the sample as an effect of chemical treatment. As observed in Fig. 4-A a, the surface of raw SCT is compact, rigid, and non-disruptive in nature. This is due to the complex binding structure of different lignocellulosic components that are interlinked with each other. It causes the recalcitrant behavior of plant cell walls, which protects the plants from degradation due to microbes and enzymes (Zoghiami and Paës 2019). This rigid structure of the raw SCT sample deteriorated (Fig. 4-A b) due to the alkali pretreatment, which removes most of the compounds, such as wax, pectin, protein, and other extractives, from the surface of the biomass along with hemicellulose and lignin. It causes defibrillation, and the fiber bundles get opened up, which allows the penetration of more alkali into the structure, resulting in cellulose swelling.

As seen in Figs. 4-A c and A d, more defibrillation and disruption of the biomass surface occurs due to the hydrogen peroxide bleaching and sulphuric acid hydrolysis. With the removal of hemicellulose and lignin, the cellulose composition increases along with the crystallinity of the sample, which results in a smoother surface than the raw SCT sample and a reduction in fiber dimensions (Ilyas et al. 2018).

Figure 4-B shows the morphology of the acid hydrolysed sample at a higher magnification level (10 μm). This figure depicts the intense disruption of the surface of the sample due to the sulphuric acid attack during hydrolysis treatment. Due to the acid hydrolysis, the cellulose microfibrils obtained after the bleaching process were disintegrated to nanoscale. In addition, with the removal of the amorphous region, the resultant material becomes highly crystalline, which was confirmed in the XRD analysis.

Thermogravimetric analysis

Fig. 5a and b show the graphical representation of thermogravimetric and derivative thermogravimetric (TGA and DTG) analysis of the raw and treated SCT samples, which indicates the thermal stability parameters of that sample. This thermal parameter depends on a few factors, such as chemical composition, structure, degree of polymerization, and degree of crystallinity of the given biomass material (Fisher et al. 2002).

As seen in Fig. 5 a, the thermal stability of the treated samples is higher compared to raw SCT. This increase in thermal stability may be due to the degradation or removal of volatile matter from the biomass during the chemical treatment. Bleached and hydrolysed samples show slightly higher thermal stability than alkali-treated samples. In Fig. 5 a, the weight loss of the material around 100 $^{\circ}\text{C}$ was due to the evaporation of the moisture content present in the sample. Then, the sudden drop in weight % in the temperature range between 250 $^{\circ}\text{C}$ to 400 $^{\circ}\text{C}$ indicates the decomposition of the major components of the biomass, such as cellulose and hemicellulose. Beyond 400 $^{\circ}\text{C}$, the change in weight % of the material was insignificant, which indicates its thermal stability with that chemical composition.

The DTG analysis in Fig. 5 b shows that the thermal decomposition of hemicellulose and cellulose for raw SCT samples starts at 210 $^{\circ}\text{C}$ and 320 $^{\circ}\text{C}$,

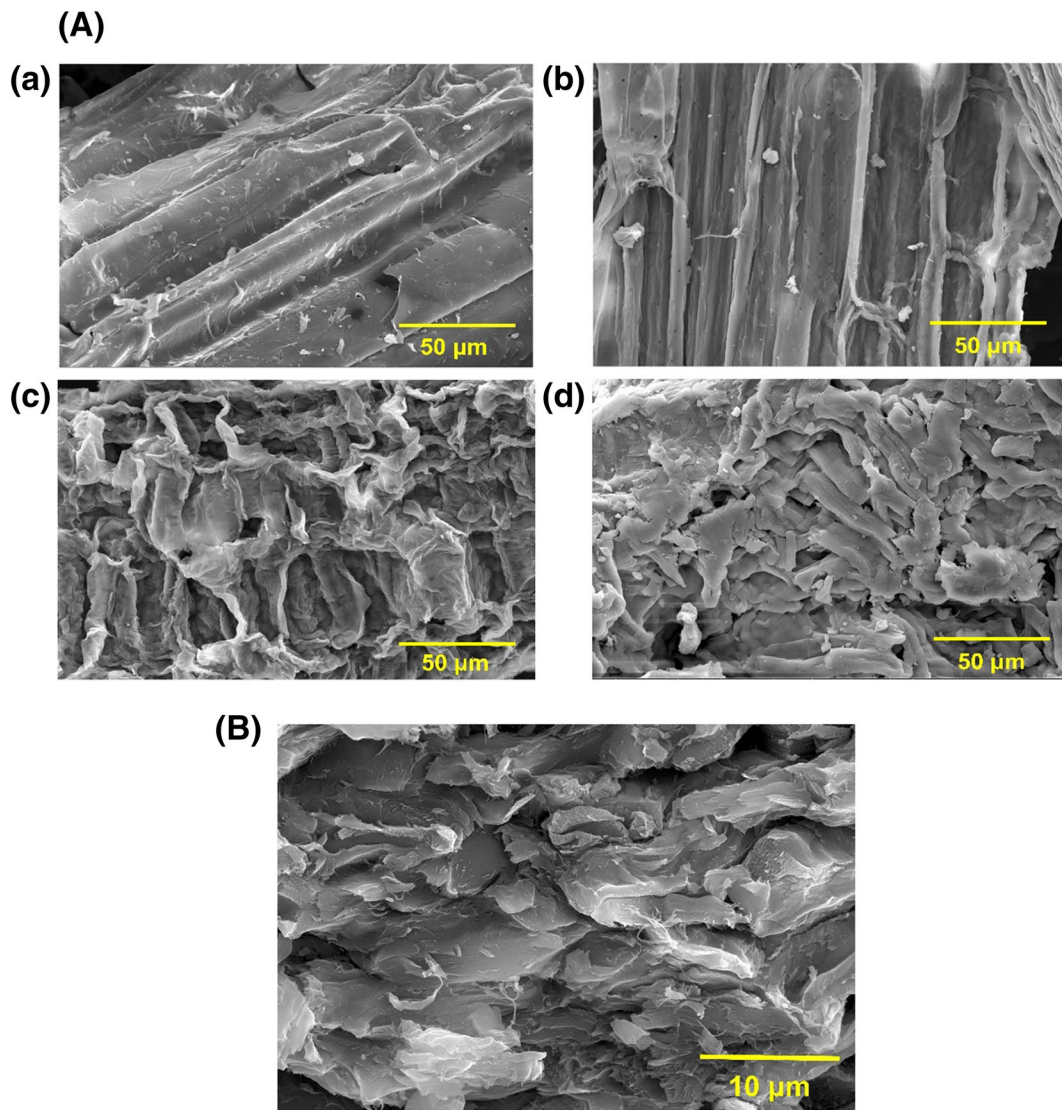


Fig. 4 A FE-SEM images of SCT samples (a) raw, (b) alkali-treated, (c) bleached, and (d) hydrolysed, B FE-SEM image of the hydrolysed sample at higher magnification

respectively. For alkali-treated biomass, the thermal degradation takes place between 250 °C to 380 °C and for bleached and hydrolysed material, this range was slightly increased to 260 °C to 400 °C, which indicates the more thermally stable behavior of the treated material due to its higher crystallinity compared to raw SCT. The higher crystallinity of the material increases its heat resistance, further improving thermal degradation.

At higher temperatures (>400 °C), the residue left consists mainly of lignin and inorganic

materials like silica, which has the highest thermal stability (Ashori et al. 2006). The weight % of this residue is higher in raw SCT than in the chemically treated samples due to the effective delignification during the pretreatment.

The kinetic parameters like activation energy (E_a) and order (n) of degradation for each of the samples at different treatment stages are estimated from the TGA data according to the method described (COATS and REDFERN 1964; Basta 1998; Basta et al. 2015; Hanna et al. 2020;

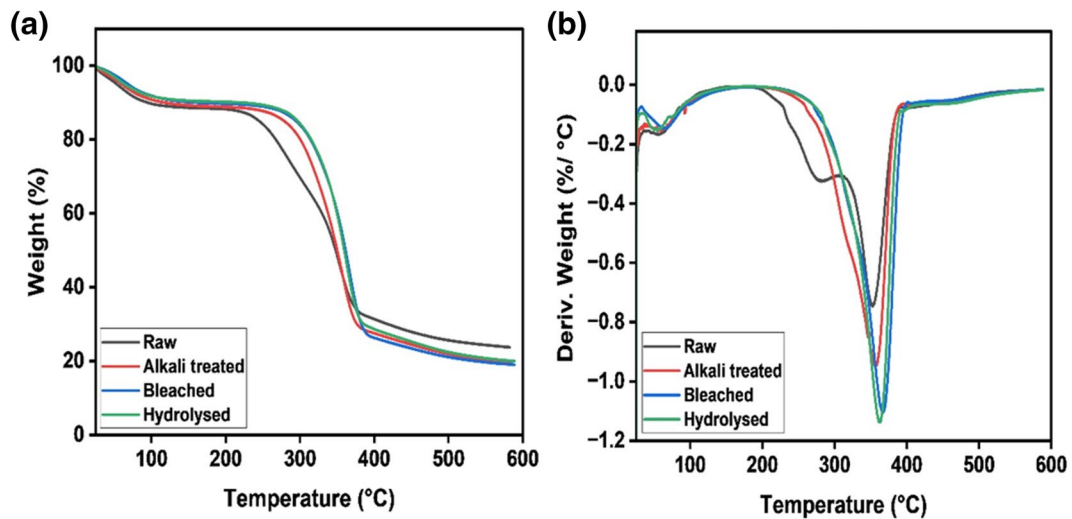


Fig. 5 a TGA and (b) DTG graphs of raw and treated SCT at different treatment stages

Khalf-Alla et al. 2021) and with the help of following Eq. 5 and 6-

For $n = 1$,

$$\ln \left[-\ln \frac{(1-\alpha)}{T^2} \right] = \ln \frac{AR}{\beta E_y} \left[1 - \frac{2RT}{E_a} \right] - \frac{E_a}{RT} \quad (5)$$

For $n \neq 1$,

$$\ln \left[\frac{1 - (1-\alpha)^{(1-n)}}{T^2(1-n)} \right] = \ln \frac{AR}{\beta E_y} \left[1 - \frac{2RT}{E_a} \right] - \frac{E_a}{RT} \quad (6)$$

Here, n is the order of degradation reaction, T is the absolute temperature (K), A is the frequency factor, β is the heating rate ($^{\circ}\text{C}/\text{minute}$), R is the universal gas constant (8.314 J/mol.K), E_a is the activation energy (kJ), and α is the fractional conversion.

The activation energy (E_a) was determined by measuring the slope of the straight line, which is obtained by plotting the values of the left-hand side of Eq. 5 and 6 depending on order (n) on the Y-axis versus $1/T$ on the X-axis. The suitable values of E_a and n are finalised by considering the value of the maximum correlation coefficient (R^2) for the corresponding straight line. The kinetic parameters thus obtained, including activation energy and order of degradation reaction at different temperature stages, along with the onset degradation temperature, DTG peak temperature, and final weight (%)

remaining for each sample, are summarised in the following Table 2.

X-ray diffraction (XRD) analysis

The X-ray diffraction pattern of raw and chemically treated SCT samples is represented in Fig. 6. The major intensity peaks observed at 2θ values of around 16° ($1 \bar{1} 0/110$ peak), 22.6° (200 peak), and 34.5° (004 peak) correspond to the crystalline nature of cellulose-I for all the samples, whereas the low-intensity region near 2θ values of about 18.6° (between the $1 \bar{1} 0/110$ peak and the 200 peak) represents the amorphous region (Segal et al. 1959; French and Santiago Cintrón 2013; French 2014).

Figure 6 shows that the intensity and sharpness of diffraction peaks for alkali-treated and bleached samples are higher than for raw SCT samples, for 2θ values around 22.6° . This is because the chemical pretreatment removes the cellulose-binding components of biomass, such as lignin and hemicellulose, which isolates the particles with a more crystalline nature. For the hydrolysed sample, a very sharp peak with maximum intensity for 2θ around 22.6° signifies the presence of a highly crystalline region as most of the amorphous part gets removed during the acid hydrolysis process.

The crystallinity index was determined for all the SCT samples at various treatment stages by

Table 2 TGA measurements of raw and treated SCT biomass

Nature of sample	Stage	Temperature range (°C)	Onset temperature (°C)	DTG peak temperature (°C)	Order, n	E _a (kJ/mol)	R ²	Weight % (Final)
Raw SCT	1st	25.23 – 126.66	256.97	56.08	-	-	-	88.941
	2nd	238.25 – 384.12		352.74	0.5	28.550	0.986	32.655
	3rd	384.12 – 582.67		408.75	1	12.485	0.837	23.742
Alkali-treated	1st	26.41 – 165.51	311.38	60.82	-	-	-	89.123
	2nd	252.65 – 381.23		357.17	0.5	37.692	0.922	29.059
	3rd	381.23 – 585.26		405.27	1	12.138	0.79	19.768
Bleached	1st	26.76 – 183.4	317.78	65.01	-	-	-	89.854
	2nd	260.38 – 403.32		366.23	2	46.209	0.952	26.09
	3rd	403.32 – 588.73		416.52	1.5	12.876	0.77	18.98
Hydrolysed	1st	25.26 – 186.28	340.74	54.16	-	-	-	90.303
	2nd	238.25 – 398.22		361.53	0.5	58.326	0.945	28.791
	3rd	398.22 – 588.73		432.36	0.5	22.099	0.999	19.984

considering the maximum and minimum intensities of diffraction peaks for all crystalline and amorphous regions shown in Fig. 6. The values of the % crystallinity index for each sample were then calculated using the Segal method (Eq. 4). The results thus obtained are summarised in Table 3, which shows that the crystallinity of the sample increases due to the chemical treatment as compared to that of the raw SCT. It indicates that there is a progressive dissolution of the amorphous part of the sample with respect to the chemical treatment, which enhances its

crystallinity (de Araújo et al. 2023). Thus, the highest crystallinity index of 84.83% was obtained for the hydrolysed sample, which implies that the major amorphous fraction of the sample gets removed by sulphuric acid treatment, and the crystalline fraction becomes resistant to the acid attack.

A similar trend of increase in CrI with the chemical treatment was observed by different researchers and reported in their literature. In the study reported by (de Araújo et al. 2023) for the nanocellulose production from cashew apple

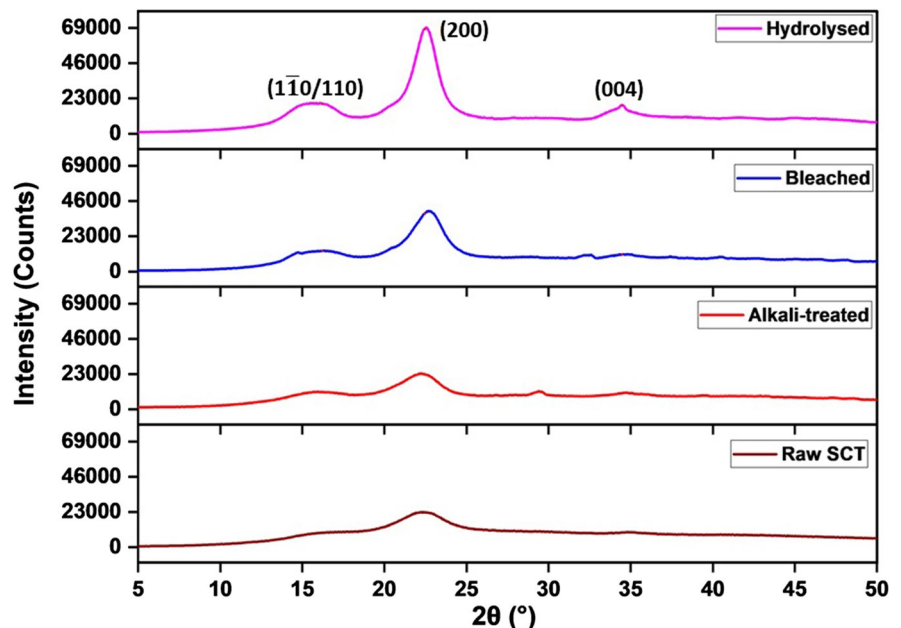
Fig. 6 X-ray diffraction patterns for raw and chemically treated SCT at different treatment stages

Table 3 The crystallinity index of raw and treated SCT biomass at optimum process conditions

Treatment stage	2 θ ($^{\circ}$) (am)	I _{am} (counts)	2 θ ($^{\circ}$) (200)	I ₂₀₀ (counts)	Crystallinity index (%)
Raw SCT	18.04	9964	22.38	23005	56.69
Alkali-treated	18.20	9305	22.22	23497	60.40
Bleached	18.52	9406	22.66	39517	76.20
Hydrolysed	18.56	10525	22.54	69390	84.83

bagasse (CAB), the CrI value increases from 51% for CAB to 71% for acid–alkali pre-treated sample (CAB-PT-HA). Similarly, in the study reported by (Akinjokun et al. 2021), the CrI (%) values increased from 33.93% for cocoa pod husk (CPH) to 63.31% for isolated cocoa pod cellulose (CPC), which further enhanced to 67.60% when CPC undergoes acid hydrolysis to form cellulose nanocrystals (CNC). In the work carried out by (Lu and Hsieh 2012), the XRD analysis shows that cellulose fibers (CF) isolated from rice straw have a CrI of 61.8%, which improves further to 86% and 91.2% due to the acid hydrolysis at different time intervals for CNC30 and CNC45 respectively. Whereas, in the case of sugarcane top biomass, the crystallinity index of the native biomass increased from 37.74% to 63.40% due to alkali-pretreatment (Sindhu et al. 2014).

It is important to note that the crystallinity index measures only the order of crystallinity of the sample and not the crystallinity of the crystalline regions (Mwaikambo and Ansell 2002).

Transmission electron microscopy (TEM)

The transmission electron micrographs of the hydrolysed SCT sample at different magnification levels (200 nm and 50 nm) are shown in Fig. 7 (a and b). It is clear from these images that the acid hydrolysed material consists of nanoparticles with a crystalline nature. These images also represent the geometry of the nanocrystalline cellulose (NCC) particles present in the given sample. The length (L) of the extracted NCC particles ranges from 100 to 260 nm with an average length of 150 nm, whereas the diameter (D) is in the range between 12 to 20 nm with an average of 16 nm. Thus, the L/D ratio for the extracted NCC present in the hydrolysed sample is around 9.375.

A comparative study with other types of biomass

The quantification and characterisation results obtained in this study are compared with some of the other biomasses reported in the literature and summarised in the following Table 4. It is observed from this comparison

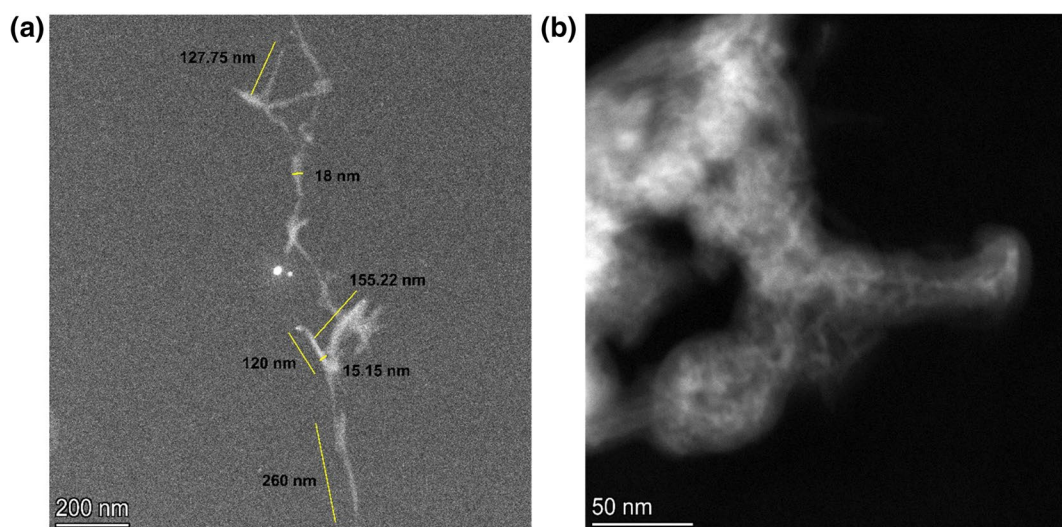
**Fig. 7** a and b TEM images of a hydrolysed SCT sample at different magnification

Table 4 Comparative study for NCC extraction from different biomasses with the present work

Sr. No	Type of biomass	Optimum conditions	2θ (°)	CrI (%)	Dimensions	Reference
1	Rice husk	65 wt.% H ₂ SO ₄ , 45 °C, 90 min	16.3, 22.4, 34.5	58.82- 76.69	L = 55.5- 778.9 nm, D = 11.7- 48.3 nm	(Rashid and Dutta 2020)
2	Rice straw	11 M H ₂ SO ₄ , 25 °C, 30 min	16.5, 22.5, 34.5	83.8	L = 100 nm, D = 10- 15 nm	(Shi and Liu 2021)
3	Sugar palm fibers	65 wt.% H ₂ SO ₄ , 45 °C, 45 min	12.3, 15, 22.1, 22.6,	85.9	L = 45- 238 nm, D = 3- 18.19 nm	(Ilyas et al. 2018)
4	Agave Angustifolia fibers	60 wt.% H ₂ SO ₄ , 45 °C, 45 min	16, 22.6, 35	82	L = 170- 500 nm, D = 8- 15 nm	(Rosli et al. 2013)
5	Apple pomace	45 wt.% H ₂ SO ₄ , 50 °C, 45 min	16.1, 22, 34.7	78	L = 28 nm, D = 7.9 nm	(Melikoglu et al. 2019)
6	Sugarcane bagasse	64 wt.% H ₂ SO ₄ , 45 °C, 60 min	16.5, 22.5, 34.6	72.5	L = 250- 480 nm, D = 20- 60 nm	(Kumar et al. 2014)
7	Sugarcane bagasse	64 wt.% H ₂ SO ₄ , 45 °C, 60 min	16.5, 22.5, 34.6	73	L = 160- 400 nm, D = 20- 30 nm	(Sofia et al. 2016)
8	Sugarcane bagasse	60% (w/v) H ₂ SO ₄ , 50 °C, 5 h	12.5, 22.5	-	L = 170 nm, D = 35 nm	(Mandal and Chakrabarty 2011)
9	Sugarcane bagasse	65 wt.% H ₂ SO ₄ , 50 °C, 40 min	18, 22.5	86	L = 89.2 ± 30.8 nm, D = 4.6 ± 1.0 nm	(Oliveira et al. 2016)
10	Sugarcane trash	40 wt.% H ₂ SO ₄ , 45 °C, 90 min	16, 22.6, 34.5	84.83	L = 100- 260 nm, D = 12- 20 nm	Present study

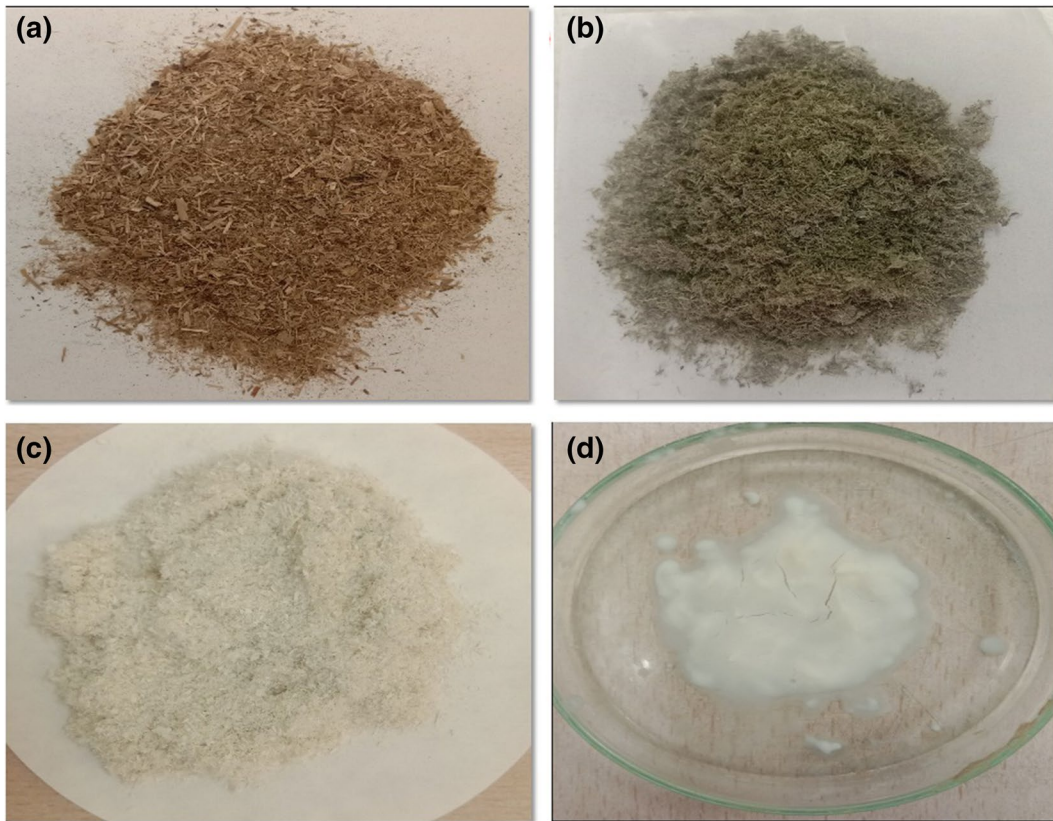


Fig. 8 Photographs of SCT samples (a) raw, b alkali treated, c bleached, and (d) hydrolysed

that the nanocrystalline cellulose was extracted effectively from various lignocellulosic biomasses. However, the optimum conditions used in the present study are substantially mild for the acid hydrolysis step for nanocrystalline cellulose from the SCT biomass but give comparable results to that for other biomasses.

Visual appearances

The compositional analysis and different characterisations of raw and chemically treated SCT confirms the progressive enrichment of cellulosic content in the material at that processing stage, but these changes can also be observed through physical appearances. Figure 8 summarises actual photographs of the SCT samples at different stages of chemical treatment, which clearly shows the changes in the colour of the material. Due to the alkali pretreatment, the dark brown colour of raw SCT turns to dark grey (Fig. 8 a and b), which further transforms into white after the bleaching process (Fig. 8

c). A white solid paste of nanocrystalline cellulose (NCC) after acid hydrolysis is observed in Fig. 8 d.

Conclusions

This paper represents the investigation results of cellulose extraction from sugarcane trash (SCT) which has still not been explored. The extraction of cellulose was carried out from SCT by using chemical treatment at mild operating conditions. The extracted cellulose microfibrils were then successfully converted into nanocrystalline cellulose (NCC) by using acid hydrolysis at a lower concentration of sulphuric acid (40 wt.%) than that reported in most of the published literature (~65 wt %). The NCC thus prepared has the potential application as a reinforcing filler in making biodegradable plastics, and for rubber and other polymeric composites.

The results of the quantification show that the chemical pretreatment at optimum process conditions enriches the biomass sample with up to 86.15% cellulose. FTIR and TGA analysis confirmed the progressive enrichment of the cellulosic groups along with the enhancement in the thermal stability of the chemically treated material than that of raw SCT. This TGA data was also helpful in determining the kinetic parameters, such as the order of degradation reaction and activation energy required at different temperature stages for each sample. The XRD study shows the crystallinity index of the material increased from 56.69% in raw SCT to 84.83% in the hydrolysed sample, whereas TEM analysis confirms the presence of nanocrystalline cellulose particles having an L/D ratio of around 9.375.

Acknowledgments The authors would like to acknowledge the support of the Management of BITS Pilani, K. K. Birla Goa Campus, and Department of Chemical Engineering for providing research and other infrastructure facilities; and Central Sophisticated Instrumentation Facility (CSIF), BITS Pilani, K. K. Birla Goa Campus and, and Advanced Facility for Microscopy and Microanalysis (AFMM), Indian Institute of Science (IISc), Bangalore for extending the support with analysis facilities.

Author's contribution Milind Joshi: Conceptualization, Visualization, Methodology, Experimental work, Writing- Original draft; Sampatrao Manjare: Supervision, Investigation, Writing- Review, & Editing.

Funding The current research received no specific grant from funding agencies in the public, commercial, or not-for-profit sectors.

Data availability The data will be made available on request.

Declarations

Ethics approval and consent to participate Not applicable.

Consent for publication Not applicable.

Competing interests The authors declare that no competing interests or other interests might be perceived to influence the results and/or discussion reported in this paper.

References

- Akinjokun AI, Petrik LF, Ogunfowokan AO et al (2021) Isolation and characterization of nanocrystalline cellulose from cocoa pod husk (CPH) biomass wastes. *Heliyon* 7:e06680. <https://doi.org/10.1016/j.heliyon.2021.e06680>
- Ashori A, Harun J, Raverty WD, MohdNMohd Y (2006) Chemical and Morphological Characteristics of Malaysian Cultivated Kenaf (*Hibiscus cannabinus*) Fiber. *Polym Plast Technol Eng* 45:131–134. <https://doi.org/10.1080/03602550500373782>
- Ballesteros I, Negro MJ, Oliva JM et al (2006) Ethanol Production From Steam-Explosion Pretreated Wheat Straw. *Appl Biochem Biotechnol* 130:496–508. <https://doi.org/10.1385/ABAB:130:1:496>
- Baruah J, Nath BK, Sharma R et al (2018) Recent Trends in the Pretreatment of Lignocellulosic Biomass for Value-Added Products. *Front Energy Res* 6:141. <https://doi.org/10.3389/fenrg.2018.00141>
- Basta AH (1998) Preparation, Characterization and Properties of Paper Sheets Made from Chemically Modified Wood Pulp Treated with Metal Salts. *Int J Polym Mater* 42:1–26. <https://doi.org/10.1080/00914039808041056>
- Basta AH, Khwaldia K, Aloui H, El-Saied H (2015) Enhancing the performance of carboxymethyl cellulose by chitosan in producing barrier coated paper sheets. *Nord Pulp Paper Res J* 30:617–625. <https://doi.org/10.3183/npprj-2015-30-04-p617-625>
- Basta AH, Lotfy VF (2023) Impact of pulping routes of rice straw on cellulose nanoarchitectonics and their behavior toward Indigo dye. *Appl Nanosci* 13:4455–4469. <https://doi.org/10.1007/s13204-022-02714-0>
- Basta AH, Lotfy VF (2023) Essential Role of Pulping Route on Thermal Stability Performance of Rice Straw-Based Nanocelluloses. *Chem Eng Technol* 46:837–847. <https://doi.org/10.1002/ceat.202200431>
- Benazzi T, Calgaroto S, Dalla Rosa C et al (2013) Hydrolysis of sugarcane bagasse using supercritical carbon dioxide to obtain fermentable sugars. *J Chem Technol Biotechnol* 88:1766–1768. <https://doi.org/10.1002/jctb.4002>
- Chieng B, Lee S, Ibrahim N et al (2017) Isolation and Characterization of Cellulose Nanocrystals from Oil Palm Mesocarp Fiber. *Polymers (basel)* 9:355. <https://doi.org/10.3390/polym9080355>
- Chotirotsukon C, Raita M, Champreda V, Laosiripojana N (2019) Fractionation of sugarcane trash by oxalic-acid catalyzed glycerol-based organosolv followed by mild solvent delignification. *Ind Crops Prod* 141:111753. <https://doi.org/10.1016/j.indcrop.2019.111753>
- Coats AW, Redfern JP (1964) Kinetic Parameters from Thermogravimetric Data. *Nature* 201:68–69. <https://doi.org/10.1038/201068a0>
- Coelho de CarvalhoBenini KC, Voorwald HJC, Cioffi MOH et al (2017) Characterization of a New Lignocellulosic Fiber from Brazil: *Imperatabrasiliensis* (Brazilian Satintail) as an Alternative Source for Nanocellulose Extraction. *J Nat Fibers* 14:112–125. <https://doi.org/10.1080/15440478.2016.1167647>
- de Araújo LGS, Rodrigues THS, Alencar LMR et al (2023) Production of nanocellulose from cashew apple bagasse: the influence of pretreatment. *Cellulose* 31(2):937–952. <https://doi.org/10.1007/s10570-023-05676-w>
- de Oliveira FB, Bras J, Pimenta MTB et al (2016) Production of cellulose nanocrystals from sugarcane bagasse fibers and pith. *Ind Crops Prod* 93:48–57. <https://doi.org/10.1016/j.indcrop.2016.04.064>
- de Oliveira JP, Bruni GP, Lima KO et al (2017) Cellulose fibers extracted from rice and oat husks and their application

- in hydrogel. *Food Chem* 221:153–160. <https://doi.org/10.1016/j.foodchem.2016.10.048>
- Ditzel FI, Prestes E, Carvalho BM et al (2017) Nanocrystalline cellulose extracted from pine wood and corncob. *Carbohydr Polym* 157:1577–1585. <https://doi.org/10.1016/j.carbpol.2016.11.036>
- Elanthikkal S, Gopalakrishnanpanicker U, Varghese S, Guthrie JT (2010) Cellulose microfibrils produced from banana plant wastes: Isolation and characterization. *Carbohydr Polym* 80:852–859. <https://doi.org/10.1016/j.carbpol.2009.12.043>
- Enriquez E, Mohanty AK, Misra M (2016) Alkali and Peroxide Bleach Treatments on Spring Harvested Switchgrass for Potential Composite Application. *Bioresources* 11:9922–9939. <https://doi.org/10.15376/biores.11.4.9922-9939>
- Fisher T, Hajjaligol M, Waymack B, Kellogg D (2002) Pyrolysis behavior and kinetics of biomass derived materials. *J Anal Appl Pyrolysis* 62:331–349. [https://doi.org/10.1016/S0165-2370\(01\)00129-2](https://doi.org/10.1016/S0165-2370(01)00129-2)
- French AD (2014) Idealized powder diffraction patterns for cellulose polymorphs. *Cellulose* 21:885–896. <https://doi.org/10.1007/s10570-013-0030-4>
- French AD, Santiago Cintrón M (2013) Cellulose polymorphy, crystallite size, and the Segal Crystallinity Index. *Cellulose* 20:583–588. <https://doi.org/10.1007/s10570-012-9833-y>
- Haghighi Mood S, Hossein Golefshan A, Tabatabaei M et al (2013) Lignocellulosic biomass to bioethanol, a comprehensive review with a focus on pretreatment. *Renew Sustain Energy Rev* 27:77–93. <https://doi.org/10.1016/j.rser.2013.06.033>
- Hanna DH, Lotfy VF, Basta AH, Saad GR (2020) Comparative evaluation for controlling release of niacin from protein- and cellulose-chitosan based hydrogels. *Int J Biol Macromol* 150:228–237. <https://doi.org/10.1016/j.ijbiomac.2020.02.056>
- Hongdan Z, Shaohua X, Shubin W (2013) Enhancement of enzymatic saccharification of sugarcane bagasse by liquid hot water pretreatment. *Bioresour Technol* 143:391–396. <https://doi.org/10.1016/j.biortech.2013.05.103>
- Hussain A, Arif SM, Aslam M (2017) Emerging renewable and sustainable energy technologies: State of the art. *Renew Sustain Energy Rev* 71:12–28. <https://doi.org/10.1016/j.rser.2016.12.033>
- Ilyas RA, Sapuan SM, Ishak MR (2018) Isolation and characterization of nanocrystalline cellulose from sugar palm fibres (Arenga Pinnata). *Carbohydr Polym* 181:1038–1051. <https://doi.org/10.1016/j.carbpol.2017.11.045>
- Intanakul P, Krairiksh M, Kitchaiya P (2003) Enhancement of Enzymatic Hydrolysis of Lignocellulosic Wastes by Microwave Pretreatment Under Atmospheric Pressure. *J Wood Chem Technol* 23:217–225. <https://doi.org/10.1081/WCT-120021926>
- Jutakanoke R, Leepipatpiboon N, Tolieng V et al (2012) Sugarcane leaves: Pretreatment and ethanol fermentation by *Saccharomyces cerevisiae*. *Biomass Bioenergy* 39:283–289. <https://doi.org/10.1016/j.biombioe.2012.01.018>
- Khalf-Alla PA, Basta AH, Lotfy VF, Hassan SS (2021) Synthesis, Characterization, Speciation, and Biological Studies on Metal Chelates of Carbohydrates with Molecular Docking Investigation. *Macromol Mater Eng* 306:2000633. <https://doi.org/10.1002/mame.202000633>
- Khan A, Jawaid M, Kian LK et al (2021) Isolation and Production of Nanocrystalline Cellulose from *Conocarpus* Fiber. *Polymers (basel)* 13:1835. <https://doi.org/10.3390/polym13111835>
- Knill CJ, Kennedy JF (2003) Degradation of cellulose under alkaline conditions. *Carbohydr Polym* 51:281–300. [https://doi.org/10.1016/S0144-8617\(02\)00183-2](https://doi.org/10.1016/S0144-8617(02)00183-2)
- Kumar A, Singh Negi Y, Choudhary V, Kant Bhardwaj N (2014) Characterization of Cellulose Nanocrystals Produced by Acid-Hydrolysis from Sugarcane Bagasse as Agro-Waste. *J Mater Phys Chem* 2:1–8. <https://doi.org/10.12691/jmpc-2-1-1>
- Kumar N, Gautam R, Stallings JD et al (2021) Secondary Agriculture Residues Pretreatment Using Deep Eutectic Solvents. *Waste Biomass Valorization* 12:2259–2269. <https://doi.org/10.1007/s12649-020-01176-1>
- Kumari D, Singh R (2018) Pretreatment of lignocellulosic wastes for biofuel production: A critical review. *Renew Sustain Energy Rev* 90:877–891. <https://doi.org/10.1016/j.rser.2018.03.111>
- Moro MK, Teixeira RSS, da Silva ASA et al (2017) Continuous pretreatment of sugarcane biomass using a twin-screw extruder. *Ind Crops Prod* 97:509–517. <https://doi.org/10.1016/j.indcrop.2016.12.051>
- Lamaming J, Hashim R, Sulaiman O et al (2015) Cellulose nanocrystals isolated from oil palm trunk. *Carbohydr Polym* 127:202–208. <https://doi.org/10.1016/j.carbpol.2015.03.043>
- Lee HV, Hamid SBA, Zain SK (2014) Conversion of Lignocellulosic Biomass to Nanocellulose: Structure and Chemical Process. *Sci World J* 2014:1–20. <https://doi.org/10.1155/2014/631013>
- Li J, Hu H, Song Y, Chai X-S (2015) New evidence for the role of the borohydride pretreatment on the hydrogen peroxide bleaching of kraft pulp. *RSC Adv* 5:98067–98074. <https://doi.org/10.1039/C5RA17964E>
- Lu P, Hsieh Y-L (2012) Preparation and characterization of cellulose nanocrystals from rice straw. *Carbohydr Polym* 87:564–573. <https://doi.org/10.1016/j.carbpol.2011.08.022>
- Mandal A, Chakrabarty D (2011) Isolation of nanocellulose from waste sugarcane bagasse (SCB) and its characterization. *Carbohydr Polym* 86:1291–1299. <https://doi.org/10.1016/j.carbpol.2011.06.030>
- Ma'ryana R, Marifatun D, Wheni AI et al (2014) Alkaline Pretreatment on Sugarcane Bagasse for Bioethanol Production. *Energy Procedia* 47:250–254. <https://doi.org/10.1016/j.egypro.2014.01.221>
- Melikoğlu AY, Bilek SE, Cesur S (2019) Optimum alkaline treatment parameters for the extraction of cellulose and production of cellulose nanocrystals from apple pomace. *Carbohydr Polym* 215:330–337. <https://doi.org/10.1016/j.carbpol.2019.03.103>
- Mishra S, Kharkar PS, Pethe AM (2019) Biomass and waste materials as potential sources of nanocrystalline cellulose: Comparative review of preparation methods (2016 – Till date). *Carbohydr Polym* 207:418–427. <https://doi.org/10.1016/j.carbpol.2018.12.004>
- Modenbach AA, Nokes SE (2014) Effects of Sodium Hydroxide Pretreatment on Structural Components of Biomass. *Trans ASABE* 57:1187–1198. <https://doi.org/10.13031/trans.57.10046>
- Mussatto SI, Rocha GJM, Roberto IC (2008) Hydrogen peroxide bleaching of cellulose pulps obtained from brewer's

- spent grain. *Cellulose* 15:641–649. <https://doi.org/10.1007/s10570-008-9198-4>
- Mwaikambo LY, Ansell MP (2002) Chemical modification of hemp, sisal, jute, and kapok fibers by alkalization. *J Appl Polym Sci* 84:2222–2234. <https://doi.org/10.1002/app.10460>
- Nacos M, Katapodis P, Pappas C et al (2006) Kenaf xylan – A source of biologically active acidic oligosaccharides. *Carbohydr Polym* 66:126–134. <https://doi.org/10.1016/j.carbpol.2006.02.032>
- Ning P, Yang G, Hu L et al (2021) Recent advances in the valorization of plant biomass. *Biotechnol Biofuels* 14:102. <https://doi.org/10.1186/s13068-021-01949-3>
- Nosratpour MJ, Karimi K, Sadeghi M (2018) Improvement of ethanol and biogas production from sugarcane bagasse using sodium alkaline pretreatments. *J Environ Manage* 226:329–339. <https://doi.org/10.1016/j.jenvman.2018.08.058>
- Oliveira FMV, Pinheiro IO, Souto-Maior AM et al (2013) Industrial-scale steam explosion pretreatment of sugarcane straw for enzymatic hydrolysis of cellulose for production of second generation ethanol and value-added products. *Bioresour Technol* 130:168–173. <https://doi.org/10.1016/j.biortech.2012.12.030>
- Owonubi SJ, Agwuncha SC, Malima NM et al (2021) Non-woody Biomass as Sources of Nanocellulose Particles: A Review of Extraction Procedures. *Front Energy Res* 9:608825. <https://doi.org/10.3389/fenrg.2021.608825>
- Powar RV, Mehete SA, Powar TR, Patil SB (2022) End-Use Applications of Sugarcane Trash: A Comprehensive Review. *Sugar Tech* 24:699–714. <https://doi.org/10.1007/s12355-022-01107-5>
- Raghavi S, Sindhu R, Binod P et al (2016) Development of a novel sequential pretreatment strategy for the production of bioethanol from sugarcane trash. *Bioresour Technol* 199:202–210. <https://doi.org/10.1016/j.biortech.2015.08.062>
- Rashid S, Dutta H (2020) Characterization of nanocellulose extracted from short, medium and long grain rice husks. *Ind Crops Prod* 154:112627. <https://doi.org/10.1016/j.indcrop.2020.112627>
- Rosli NA, Ahmad I, Abdullah I (2013) Isolation and characterization of cellulose nanocrystals from agave angustifolia fibre. *BioResources* 8(2):1893–1908. <https://doi.org/10.15376/biores.8.2.1893-1908>
- Sain M, Panthapulakkal S (2006) Bioprocess preparation of wheat straw fibers and their characterization. *Ind Crops Prod* 23:1–8. <https://doi.org/10.1016/j.indcrop.2005.01.006>
- Seddiqi H, Oliaei E, Honarkar H et al (2021) Cellulose and its derivatives: towards biomedical applications. *Cellulose* 28:1893–1931. <https://doi.org/10.1007/s10570-020-03674-w>
- Segal L, Creely JJ, Martin AE, Conrad CM (1959) An Empirical Method for Estimating the Degree of Crystallinity of Native Cellulose Using the X-Ray Diffractometer. *Text Res J* 29:786–794. <https://doi.org/10.1177/004051755902901003>
- Shi S-C, Liu G-T (2021) Cellulose nanocrystal extraction from rice straw using a chlorine-free bleaching process. *Cellulose* 28:6147–6158. <https://doi.org/10.1007/s10570-021-03889-5>
- Sindhu R, Kuttiraja M, Binod P et al (2014) Physicochemical characterization of alkali pre-treated sugarcane tops and optimization of enzymatic saccharification using response surface methodology. *Renew Energy* 62:362–368. <https://doi.org/10.1016/j.renene.2013.07.041>
- Singh P, Suman A, Tiwari P et al (2008) Biological pretreatment of sugarcane trash for its conversion to fermentable sugars. *World J Microbiol Biotechnol* 24:667–673. <https://doi.org/10.1007/s11274-007-9522-4>
- Singh SP, Jawaid M, Chandrasekar M et al (2021) Sugarcane wastes into commercial products: Processing methods, production optimization and challenges. *J Clean Prod* 328:129453. <https://doi.org/10.1016/j.jclepro.2021.129453>
- Sofla MRK, Brown RJ, Tsuzuki T, Rainey TJ (2016) A comparison of cellulose nanocrystals and cellulose nanofibres extracted from bagasse using acid and ball milling methods. *Adv Nat Sci: Nanosci Nanotechnol* 7:035004. <https://doi.org/10.1088/2043-6262/7/3/035004>
- Sun J-X, Sun R, Sun X-F, Su Y (2004) Fractional and physicochemical characterization of hemicelluloses from ultrasonic irradiated sugarcane bagasse. *Carbohydr Res* 339:291–300. <https://doi.org/10.1016/j.carres.2003.10.027>
- Talha Z, Ding W, Mehryar E et al (2016) Alkaline Pretreatment of Sugarcane Bagasse and Filter Mud Codigested to Improve Biomethane Production. *Biomed Res Int* 2016:1–10. <https://doi.org/10.1155/2016/8650597>
- Van Soest PJ, Robertson JB, Lewis BA (1991) Symposium: carbohydrate methodology, metabolism and nutritional implications in dairy cattle methods for dietary fiber, neutral detergent fiber and nonstarch polysaccharides in relation to animal nutrition. *J Dairy Sci (EUA)* 74(10):3583–3597
- Velmurugan R, Muthukumar K (2011) Utilization of sugarcane bagasse for bioethanol production: Sono-assisted acid hydrolysis approach. *Bioresour Technol* 102:7119–7123. <https://doi.org/10.1016/j.biortech.2011.04.045>
- Wahib SA, Da'na DA, Al-Ghouti MA (2022) Insight into the extraction and characterization of cellulose nanocrystals from date pits. *Arab J Chem* 15:103650. <https://doi.org/10.1016/j.arabjc.2021.103650>
- Yogalakshmi KN, Sivashanmugam P et al (2022) Lignocellulosic biomass-based pyrolysis: A comprehensive review. *Chemosphere* 286:131824. <https://doi.org/10.1016/j.chemosphere.2021.131824>
- Yu B, Fan G, Zhao S et al (2021) Simultaneous isolation of cellulose and lignin from wheat straw and catalytic conversion to valuable chemical products. *Appl Biol Chem* 64:15. <https://doi.org/10.1186/s13765-020-00579-x>
- Zhang H, Zhang S, Yuan H et al (2018) FeCl₃-catalyzed ethanol pretreatment of sugarcane bagasse boosts sugar yields with low enzyme loadings and short hydrolysis time. *Bioresour Technol* 249:395–401. <https://doi.org/10.1016/j.biortech.2017.10.053>
- Zoghلامي A, Paës G (2019) Lignocellulosic Biomass: Understanding Recalcitrance and Predicting Hydrolysis. *Front Chem* 7:874. <https://doi.org/10.3389/fchem.2019.00874>

Publisher's Note Springer Nature remains neutral with regard to jurisdictional claims in published maps and institutional affiliations.

Springer Nature or its licensor (e.g. a society or other partner) holds exclusive rights to this article under a publishing agreement with the author(s) or other rightsholder(s); author self-archiving of the accepted manuscript version of this article

is solely governed by the terms of such publishing agreement and applicable law.